

A 3-DIMENSIONAL STUDY OF THE LOCAL ENVIRONMENT OF BRIGHT IRAS GALAXIES: THE AGN/STARBURST CONNECTION.

ELIAS KOULOURIDIS^{1,3}, VAHRAM CHAVUSHYAN^{2,4}, MANOLIS PLIONIS^{1,2}, YAIR KRONGOLD⁴, AND DEBORAH DULTZIN-HACYAN⁴

Draft version June 29, 2018

ABSTRACT

We present a 3-dimensional study of the local ($\leq 100 h^{-1}$ kpc) and the large scale ($\leq 1 h^{-1}$ Mpc) environment of Bright IRAS Galaxies (BIRGs). For this purpose we use 87 BIRGs located at high galactic latitudes (with $0.008 \leq z \leq 0.018$) as well as a control sample of non-active galaxies having the same morphological, redshift and diameter size distributions as the corresponding BIRG sample. Using the Center for Astrophysics (CfA2) and Southern Sky Redshift Survey (SSRS) galaxy catalogues ($m_b \lesssim 15.5$) as well as our own spectroscopic observations ($m_b \lesssim 19.0$) for a subsample of the original BIRG sample, we find that the fraction of BIRGs with a close neighbor is significantly higher than that of their control sample. Comparing with a related analysis of Sy1 and Sy2 galaxies of Koulouridis et al. (2006) we find that BIRGs have a similar environment as Sy2s, although the fraction of BIRGs with a bright close neighbor is even higher than that of Sy2 galaxies. An additional analysis of the relation between FIR colors and the type of activity of each BIRG shows a significant difference between the colors of strongly-interacting and non-interacting starbursts and a resemblance between the colors of non-interacting starbursts and Sy2s. Our results support the view where close interactions can drive molecular clouds towards the galactic center, triggering starburst activity and obscuring the nuclear activity. When the close neighbor moves away, starburst activity is reduced with the simultaneous appearance of an obscured (type 2) AGN. Finally, the complete disentanglement of the pair gives birth to an unobscured (type 1) AGN.

Subject headings: galaxies: — active — infrared — starburst: galaxies: — large-scale structure of the universe

1. INTRODUCTION

The IRAS Revised Bright galaxy sample by Sanders et al. (2003) includes all galaxies with total $60 \mu\text{m}$ flux density greater than 5.24 Jy . The sample is the result of a highly complete flux-limited survey conducted by IRAS covering the entire sky at galactic latitudes $|b| \geq 5^\circ$ and was compiled after the final calibration of the IRAS Level 1 Archive. It offers far more accurate and consistent measurements of the flux of objects with extended emission. In addition, the infrared fluxes of over 100 sources from the sample were recalculated by the IRAS High Resolution (HIRES) processing, which allowed the deconvolution of close galaxy pairs (Surace, Sanders, Mazarella 2004). The latter provides a more-than-ever reliable database of the IRAS galaxies which can be proved crucial for statistical studies like this one.

While the relation between Ultra Luminous IRAS Galaxies (ULIRGs) and strong interactions has been thoroughly studied (e.g. Sanders, Surace & Ishida 1999, Wang et al. 2006), this is not the case for the environment of moderately and low luminous infrared galaxies. A 2-dimensional analysis of Krongold et al. (2002) showed a trend for a Bright IRAS Galaxy (BIRG) sample on having neighbors in excess of normal galaxies and

Sy1 galaxies, but in relative agreement with Sy2 galaxies. However, the BIRG population consists of various types of active galaxies, including starbursts (the majority), Seyferts, Liners and normal galaxies and thus it would be of great interest to clarify the connection between infrared emission, interactions and different types of active galaxies.

During the last decade, many studies have investigated the relation among interacting galaxies, starbursting and nuclear activity (eg. Hernandez-Toledo et al. 2001; Ho 2005). Despite the plethora of available information, searches for correlations between the above physical processes are inconclusive, the only exception being the coupling between interactions and starbursting. However, there is evidence that AGN galaxies host a post-starburst stellar population (eg. Boisson et al. 2000, González Delgado et al. 2001) while Kauffmann et al. (2003) showed that the fraction of post-starburst stars increases with AGN emission. Proving a relation of this type between starburst and AGN galaxies would simultaneously solve also the problem of the AGN triggering mechanism. Interactions would be the main cause of such activities, being starbursting and/or the feeding of a central black hole. However, this is not a trivial task. The main difficulty arises from the fact that the Star Formation Rate (SFR) estimation in AGN host galaxies is still problematic. All SFR estimation methods present complications and even those based on the FIR continuum are doubtful, since the contribution of the active nuclei is unknown (eg. Ho 2005).

Despite the difficulties, some studies, based on different diagnostics seem to conclude that there is indeed an

¹ Institute of Astronomy & Astrophysics, National Observatory of Athens, I. Metaxa & B. Pavlou, P. Penteli 152 36, Athens, Greece

² Instituto Nacional de Astrofísica Óptica y Electrónica, A.P. 51 y 216, C.P. 72000, Puebla, Pue., México

³ Physics Department, Univ. of Patras, Panepistimioupolis Patras, 26500, Patras, Greece

⁴ Instituto de Astronomía, Universidad Nacional Autónoma de México, A.P. 70-264, México, D. F. 04510, México

evolutionary sequence from starburst to type 2 and then to type 1 AGN galaxies (e.g. Oliva et al. 1999, Krongold et al. 2002). In addition, Kim, Ho and Im (2006), using the [OII] emission line as a SFR indicator, reach the conclusion that type 2 are the precursors of type 1 quasars supporting the previous claims. These studies are based on the observed differences between different types of AGNs and resemblance of type 2 objects to starbursts. This raises doubts about the simplest version of the unification scheme of AGNs. It is true that the recent discovery of $10\mu\text{m}$ silicate emission in two luminous quasars implies the presence of dust, but it is not clear yet what is the spatial distribution of this material (Siebenmorgen et al. 2005). In addition, silicate emission is not yet detected in other type 1 objects and thus more observations are needed to establish the existence of the dusty torus.

We can summarize all the previous in two statements: (1) the starburst-AGN connection is still not well established and (2) the AGN unification model, although successful in interpreting many observational facts, remains fragile. From our point of view, our BIRG sample offers a homogeneous and complete database, which is ideal for a statistical study on these issues.

We will discuss our galaxy samples in section §2. Our data analysis and results will be presented in §3, while in section §4 we will discuss our results and present our conclusions. Due to the fact that all our samples are local, cosmological corrections of galaxy distances are negligible. Throughout our paper we use $H_0 = 100 h$ Mpc.

2. OBSERVATIONS & SAMPLES

2.1. BIRG Galaxies and Control Sample

The Bright IRAS sample consists of 87 objects with redshifts between 0.008 and 0.018 and was compiled from the BIRG survey by Soifer et al. (1989) for the northern hemisphere and by Sanders et al. (1995) for the southern. It includes only high galactic latitude objects ($|b| > 30^\circ$) in order to avoid extinction and confusion with galactic stars. All objects lay in the luminosity range of $10^{10} h^{-2} L_\odot \leq L_{\text{FIR}} \leq 10^{12} h^{-2} L_\odot$. This sample is volume limited and a V/V_{max} test gives a value of 0.47 ± 0.05 . Since the BIRG survey is highly complete, this sample is expected to be as well. More details about the sample selection are given in Krongold et al. (2002). In addition we have refined the Bright IRAS sample by correcting the infrared fluxes using “The IRAS Revised Bright Galaxy Sample” by Sanders et al. (2003). Furthermore for interacting galaxies we used the corrected fluxes given by Surace, Sanders and Mazzarella (2004).

We also use the control sample, compiled by Krongold et al. (2002) in such a way as to reproduce the main characteristics, other than the infrared emission, of the Bright IRAS sample. Specifically, the control sample was compiled from the original CfA catalog to reproduce closely the redshift, morphological type and diameter size distributions of the corresponding IRAS sample. In other words, the selection of the IRAS sample and its corresponding control sample is exactly the same, the only difference being the infrared luminosity. This is very important in order to validate that any possible environmental effect is related to the mechanisms that produce the observed high infrared luminosity and not to possible differences in the host galaxies or sample biases.

In Table 1 we present the names, celestial coordinates, Zwicky magnitudes, redshifts nearest neighbor projected linear distance and spectral types of our final list of Bright IRAS galaxies.

2.2. SSRS and CfA2 catalogues

In order to investigate the local and large scale environment around our BIRG and control sample galaxies we use the CfA2 and SSRS galaxy catalogues which cover a large solid angle of the sky. Although these galaxy catalogues date from the 80’s and 90’s they still provide an important database for studies of the properties of galaxies and their large-scale distribution in the nearby Universe. We briefly present the main characteristics of these catalogues.

The CfA2 redshift catalog contains approximately 18000 galaxy redshifts in the northern sky down to a magnitude limit of $m_B = 15.5$ (Huchra 1990). The magnitude system used is the merging of the original Zwicky magnitudes and the more accurate RC1 $B(0)$ magnitudes. These exhibit a scatter of ~ 0.3 mags (eg. Bothun & Cornell 1990). Following Huchra (1990), we do not attempt to translate these magnitudes to a standard photometric system since this requires accurate knowledge of the morphological type and size of each individual galaxy.

The SSRS catalog (da Costa et al. 1998) contains redshifts, B magnitudes and morphological classifications for ~ 5400 galaxies in two regions covering a total of 1.70 steradians in the southern celestial hemisphere and it is more than 99% complete down to $m_B = 15.5$. The galaxies have positions accurate to about 1 arcsec and magnitudes with an rms scatter of about 0.3 mag. The radial velocity precision is of ~ 40 km/s.

Note that in the regions covered by the SSRS and CfA2 catalogues, only a subsample of the original BIRGs and their control samples can be found (76 Bright IRAS galaxies and 61 control galaxies). In order to test whether these subsamples are statistically equivalent with their parent samples (ie., their diameter, morphological type and redshift distributions) we used the Kolmogorov-Smirnov two-sample test. We verified that the null hypothesis, the subsamples being equivalent with their parent samples, cannot be rejected at any significant statistical level.

2.3. Our spectroscopic observations

In order to cover a larger magnitude difference between the BIRGs and their nearest neighbor than that imposed by the CfA2/SSRS magnitude limit ($m_B \sim 15.5$) we have obtained our own spectroscopic observations of fainter neighbors around a subsample of our BIRGs, consisting of 24 galaxies (selected randomly from their parent sample). Around each BIRG we have obtained spectra of all neighboring galaxies within a projected radius of $100 h^{-1}$ kpc and a magnitude limit of $m_B \lesssim 19.0$.

Our aim with this new fainter neighbor search is not to establish or not the existence of close neighbors around the BIRGs. This will be done by using the brighter SSRS and CfA2 catalogues, at the magnitude limit of which we have well defined control samples. What we seek with these observations is to facilitate a comparison with a similar analysis of Seyfert galaxies by Koulouridis et al. (2006), in which Sy2’s were found to have significantly higher fraction of neighbors with respect to Sy1’s. In

other words we wish to establish whether the fractional differences in-between the Sy1, Sy2 and BIRG samples of galaxies, already determined (or not) as significant with respect to their control samples, continue to fainter magnitudes.

Optical spectroscopy was carried out using the Faint Object Spectrograph and Camera (LFOSC) (Zickgraf et al. 1997) mounted on the 2.1m Guillermo Haro telescope in Cananea, operated by the National Institute of Astrophysics, Optics and Electronics (INAOE) of Mexico. A setup covering the spectral range 4200 – 9000 Å with a dispersion of 8.2 Å/pix was adopted. The effective instrumental spectral resolution was about 18 Å. The data reduction was done using the IRAF packages and included bias and flat field corrections, cosmic ray cleaning, wavelength linearization, and flux transformation.

In Table 2 we present the BIRG name, coordinates, redshift and magnitude for this subsample of BIRGs. Below the row of each BIRG we list the corresponding data for all its neighbors, within a projected separation of 100 h^{-1} kpc. Since Zwicky magnitudes were not available for the fainter neighbors and in order to provide a homogeneous magnitude system for all the galaxies we decided to list in Table 2 the O_{MAPS} magnitudes⁵ for all galaxies, being the central BIRG or their neighbors (see <http://aps.umn.edu/docs/photometry>). The neighbor measured redshift is presented in the fifth column (while in some very few cases we list the redshift from the NED). The uncertainties listed are estimated from the redshift differences which result from using different emission lines.

3. ANALYSIS AND RESULTS

We search for the nearest neighbor around each BIRG and control galaxy in our samples with the aim of estimating the fraction of BIRG and normal galaxies that have a close neighbor. To define the neighborhood search we use two parameters, the projected linear distance (D) and the radial velocity separation (δv) between the central BIRG and the neighboring galaxies found in the CfA2 and SSRS catalogues or in our own spectroscopic observations. We search for neighbors with $\delta v \leq 600$ km/s, which is roughly the mean galaxy pairwise velocity of the CfA2 and SSRS galaxies or about twice the mean pairwise galaxy velocity when clusters of galaxies are excluded (Marzke et al. 1995). Note however that our results remain robust even for $\delta v \leq 1000$ km/s. We then define the fraction of BIRG and normal galaxies that have their nearest neighbor within the selected δv separation, as a function of increasing D .

3.1. Neighbors with $m_B \lesssim 15.5$ (CfA2 & SSRS)

In Figure 1 (upper panels) we plot the fraction of BIRG and control galaxies as a function of the projected distance (D) of the first companion and for two velocity separations ($\delta v \leq 200$ km/s and $\delta v \leq 600$ km/s). For comparison we also plot the results of a similar analysis by Koulouridis et al. (2006) concerning Seyfert galaxies and their control samples.

It is evident that a significantly higher fraction of BIRG galaxies have a near neighbor within $D \lesssim 100 h^{-1}$ kpc

with respect to their control sample. In Koulouridis et al. (2006) we found that there is a significantly higher fraction of Sy2 galaxies ($\sim 27\%$) having a near neighbor within $D \lesssim 75 h^{-1}$ kpc with respect to both their control sample and the Sy1 galaxies ($\sim 14\%$). Adding here the BIRG sample, which includes mostly starburst and Sy2 galaxies (see Table 1), we can clearly see that an even higher fraction of BIRGs ($\sim 42\%$) tend to have a close companion within $D \lesssim 75 h^{-1}$ kpc. The latter needs a further explanation since it is not consistent with most starburst-AGN connection scenarios, which suggest a simultaneous creation of starburst and Sy2 nuclei triggered by interactions.

In order to investigate whether fainter neighbors, than those found in the relatively shallow CfA2 and SSRS catalogues, exist around our BIRGs, we have performed a spectroscopic survey of all neighbors with $m_B \lesssim 19.0$ ($\gtrsim 3$ magnitudes fainter than the CfA2 and SSRS limits). This limit translates into an absolute magnitude limit of $M_B \sim -15.2$ for the most distant objects in our sample ($z = 0.018$). This magnitude is fainter even than that of the Small Magellanic Cloud.

3.2. Neighbors with $m_B \lesssim 19.0$ (our spectroscopy)

Here we present results of our spectroscopic observations of all the neighbors with $D \leq 75 h^{-1}$ kpc and $m_B \lesssim 19.0$ for the subsample of 24 BIRG galaxies (see Table 2).

We find that in total 13 out of the 24 BIRGs have at least one close neighbor within the above limits, with 9 of these having neighbors already detected in the SSRS and CfA2 catalogues, i.e., only 4 BIRGs have fainter than $m_b \sim 15.5$ neighbors. This implies that the BIRGs having a close neighbor (within $D \leq 75 h^{-1}$ kpc and for $\delta v \leq 600$ km/s) increases only by $\sim 45\%$ when going fainter.

Koulouridis et al. (2006) showed that the percentage of both Sy1 and Sy2 galaxies that have a close neighbor (within the above limits) increases correspondingly by about 100% when we descent from $m_B \lesssim 15.5$ to $m_B \lesssim 19.0$ (but remember that the host galaxies have magnitudes slightly closer to the CfA2 and SSRS limit). In detail, while the percentage of Sy1 and Sy2 galaxies having a close neighbor increases from 14% to 27% and from 27% to 55% respectively, for BIRGs it increases from 42% to 54%, reaching the equivalent Sy2 levels. We summarize that BIRGs, with respect to their control sample, show an excess of close neighbors which therefore should be responsible for their excess FIR emission. These results confirm a previous 2-dimensional analysis of Krongold et al. (2002) of the same BIRG sample.

Since the fractions of both BIRGs and Sy2s that have a close neighbor is roughly the same, an interesting question is whether there are any magnitude differences between hosts and neighbors for the BIRGs and the Sy2s. In Figure 2 we present the distribution of such magnitude differences (Δm) between hosts and nearest neighbor for the BIRGs and the Sy2s. Although there appears to be a slight preference for brighter neighbors of the BIRGs with respect to the Sy2s, the two distributions are statistically equivalent, as quantified by a K-S test which gives a probability of them being drawn from the same parent population of ~ 0.75 .

⁵ O (blue) POSS I plate magnitudes of the Minnesota Automated Plate Scanner (MAPS) system.

3.3. Large scale environmental analysis

Here we investigate whether there are differences in the large scale environment of BIRGs with respect to their control galaxies and to the Sy1 and Sy2 samples of Koulouridis et al. (2006). To this end we determine the galaxy overdensity, based on the CfA2 and SSRS catalogues, in a region around each BIRG or control sample galaxy. We count all neighboring galaxies around each galaxy within a projected radius of $1 h^{-1}$ Mpc, while to take into account the galaxy peculiar velocities, we use a radial velocity separation of $\delta v \leq 1000$ km/s.

We estimate the expected CfA2 and SSRS field galaxy density, $\langle \rho \rangle$, at the distance of each galaxy by integrating the corresponding CfA2 or SSRS luminosity function (Marzke, Huchra & Geller 1994; da Costa et al. 1994) using as a lower integration limit the minimum galaxy luminosity that corresponds to the galaxy catalogue magnitude limit (ie., $m_B = 15.5$) at that distance. We then compute the local overdensity around each AGN, within the previously mentioned cylinder, which is given by: $\Delta \rho = (\rho - \langle \rho \rangle) / \langle \rho \rangle$, where $\rho = N/V$ with N the number of neighbors and V the corresponding volume of the cylinder.

In Figure 3 we plot the overdensity frequency distribution for the BIRGs (left panel) and the corresponding distribution of their control galaxy sample. For comparison, we also plot the distributions for the Seyfert galaxies of Koulouridis et al. (2006). A Kolmogorov-Smirnov test shows that there is no statistically significant difference between any active galaxy sample (BIRG or Seyfert) and their respective control sample distribution.

However, there is a statistically significant difference, at a 0.03 and 0.09 level, between the overdensity distributions of BIRGs - Sy1s and Sy1s - Sy2s, respectively. Similar, differences are also found between their respective control samples. On the other hand the corresponding distributions of BIRGs and Sy2s (and of their control samples) are statistically equivalent at a 0.9 level. This implies that the large scale environment of BIRGs and Sy2s is similar but significantly different to that of Sy1s, a difference which since it is also seen in their corresponding control samples should be attributed to differences of the host galaxies. Indeed, Sy1 hosts are earlier type galaxies (e.g., Hunt & Malkan 1999, Koulouridis et al. 2006) which are known to be more clustered than late types (e.g., Willmer et al. 1998).

3.4. FIR color analysis

In these section we investigate whether there is relation between the strength of the interaction of BIRGs with their closest neighbor and their FIR characteristics. The strength of any interaction could be parametrized as a function of the distance between the BIRG and its first neighbor. At this first order analysis we do not take into account the magnitude difference between BIRGs and their close neighbor, which as we have shown previously (see figure 2), does not appear to be significantly differ from that of Sy2 galaxies. We divided the interactions in our sample into three categories based on the proximity of the first neighbor. We consider strong interactions when $D \leq 30 h^{-1} \text{ kpc}$, weak interactions when $30 \leq D \leq 100 h^{-1} \text{ kpc}$ and no interaction when $D > 100 h^{-1} \text{ kpc}$.

In Figure 4 we present the color - color diagram of

$\alpha(60, 25)$ versus $\alpha(25, 12)$, where $\alpha(\lambda_1, \lambda_2)$ is the spectral index defined as $\alpha(\lambda_1, \lambda_2) = \log(S_{\lambda_1}/S_{\lambda_2})/(\lambda_2/\lambda_1)$ with S_{λ_1} the flux in janskys at wavelength λ_1 . We can clearly see the differences between the FIR characteristics among different types of galaxies and different interaction strengths. The different interaction strengths are coded by different types of symbols while the different activity is color coded as indicated in the caption of the figure. We cross-identified classifications of each BIRG combining various studies like : The Pico Dos Dias Survey (Coziol et al. 1998), Optical Spectroscopy of luminous infrared galaxies (Veilleux et al. 1997; Ho, Filippenko, Sargent 1995), COLA - Radio and spectroscopic diagnostics of nuclear activity in galaxies (Corbett et al. 2002), Warm Iras Sources (de Grijp et al. 1987) and, when available, SDSS spectroscopic data.

It is evident that the FIR characteristics of starburst galaxies in our BIRG sample differ significantly depending on the strength of the interaction. The majority of highly interacting starburst have $\alpha(60, 25)$ spectral indices greater than -2, while all, except one, non-interacting starbursts have less. We also find that normal galaxies and Liners are at the lower end of this sequence. The only highly-interacting starburst galaxy below $\alpha(60, 25) = -2.15$ is NGC7541 which happens to have more than two times the typical molecular gas mass of BIRGs (Mirabel & Sanders 1988). The difference between highly interacting and non-interacting starburst galaxies, as quantified by a K-S test, is significant at a $> 99.9\%$ level when comparing their $\alpha(60, 25)$ index distribution. However, Sy2 galaxies, interacting or no, seem to lay in the same area ($-2.5 < \alpha(60, 25) < -2$) with non-interacting starburst galaxies, delineated in figure 4 by blue dashed lines.

The FIR color analysis of our sample strengthens our previous results. It clearly shows that the starburst activity is higher when interactions are stronger and ceases when the interacting neighboring galaxy moves away. While the starburst activity weakens (if we link position on the plot with time) Sy2 nuclei appear, giving further evidence on the causal bridging between these objects.

4. DISCUSSION & CONCLUSIONS

We have compared the 3-dimensional environment of a sample of local BIRGs with that of a well defined control sample, selected in such a way as to reproduce the redshift, morphological type and diameter size distributions of the BIRG sample. We searched for close neighbors around each BIRG and control sample galaxy using the distribution of CfA2 and SSRS galaxy catalogues as well as our own spectroscopic observations reaching a fainter magnitude limit (but for a restricted BIRG subsample). We also compared our results with those of a similar analysis of Seyfert galaxies (Dultzin-Hacyan et al. 1999; Koulouridis et al. 2006).

We find that the fraction of BIRG galaxies having a close neighbor, within a projected separation of $75 h^{-1} \text{ kpc}$ and radial velocity difference of $\delta v \leq 600$ km/s, is significantly higher than the corresponding fraction of its control sample and that of Sy1 galaxies while it is comparable to that of Sy2 galaxies. This result is in accordance with some previous two-dimensional studies (eg. Krongold et al. 2002). We reach similar results regarding the large scale environment of BIRGs (within

a projected radial separation of $1 h^{-1}$ Mpc and a radial velocity difference $\delta v \leq 1000$ km/s). Once more their behavior resembles that of Sy2's but not of Sy1's. We also find a statistically significant difference between highly-interacting and non-interacting BIRGs, based on their FIR color properties. Sy2s appear to display a similar behavior to that of non-interacting starburst galaxies, introducing new evidence for the starburst/AGN connection scenarios.

Our results can be accommodated in a simple evolutionary scenario, starting with an interaction, and ending in a Sy1 phase. First, close interactions would drive molecular clouds towards the central area, creating a circumnuclear starburst. Then, material could fall even further into the innermost regions of the galaxy, feeding the black hole, and giving birth to an AGN which at first cannot be observed due to obscuration. At this stage only a starburst would be observed. As starburst activity relaxes and obscuration decreases, a Sy2 nucleus would be revealed (still obscured by the molecular clouds from all viewing angles). As a final stage, a Sy1 phase could appear. In this case, the molecular clouds, initially in a spheroidal distribution, could flatten and form a "torus" (as in the unification scheme for Seyferts). As more material is accreted, it is possible that the AGN strengthens driving away most of the obscuring clouds, and leaving a "naked" Sy1 nuclei.

If indeed interactions play a role in triggering activity, as suggested by the above picture, then the lack of close companions among Sy1 galaxies implies that the time needed for type 1 activity to appear should be larger than the timescale for an unbound companion to escape from the close environment, or comparable to the timescale needed for an evolved merger ($\sim 10^9$ years, see Krongold et al. 2002).

It should be noted that the evolutionary scenario does not contradict the unification scheme. It implies that Sy1s and Sy2s are the same objects (as the unification model proposes) but not necessarily at the same evolutionary phase. However, there could be a phase where only orientation could define if an object appears as a Sy1 or as a Sy2, which is the stage where molecular clouds form a torus but have not been swept away yet.

Evidently, more detailed observations of large samples of galaxies are needed to resolve this important issue. However, such a picture is consistent with the evolution-

ary scenario suggested by Tran (2003). He studied a sample of Sy2 in polarized light, and found that only 50% of them showed the presence of a hidden broad line region (HBLR). He suggested that non-HBLR Sy2 galaxies could evolve into HBLR Sy2 galaxies. In this case, the appearance of the BLR could be related to the accretion rate (e.g. Nicastro 2000), and thus with the evolutionary stage of the object. The trend is also consistent with the finding that 50% of Sy2 galaxies also show the presence of a strong starburst (Gu et al. 2001; Cid-Fernandez et al. 2001).

On the brightest end, there is also growing evidence showing (a) that ULIRGs can be the precursors of quasars and (b) ULIRGs are found in very strong interacting systems or in mergers (e.g. Sanders, Surace and Ishida 1999; Wang et al. 2006). Therefore, the evolutionary sequence proposed above could be general to all nuclear activity and independent on luminosity (we note that Krongold et al. 2003 suggested a similar scheme for LINERs that can be considered as the very low luminosity extension of the evolutionary model suggested here). Further evidence comes from the fact that type 2 quasars also tend to be in interaction more often than type 1 quasars (Serber et al. 2006).

In order to better understand the role of interactions in driving starburst and nuclear activity (and the validity of the evolutionary trend), we are in the process of studying AGN and starburst manifestations in the nearest neighbors of the active galaxies in our samples, since the same physical processes should act on both members of the pair (host and nearest neighbor).

EK thanks the IA-UNAM for its warm hospitality were a major part of this work was completed. MP acknowledges funding by the Mexican Government research grant No. CONACyT 39679, VC by the CONACyT research grants 39560-F, 42609 and D. D-H support from grant IN100703 from DGAPA, PAPIIT, UNAM. This research has made use of the MAPS Catalog of POSS I supported by the University of Minnesota (the APS databases can be accessed at <http://aps.umn.edu/>) and of the USNOFS Image and Catalogue Archive operated by the United States Naval Observatory, Flagstaff Station (<http://www.nofs.navy.mil/data/fchpix/>).

REFERENCES

- Boisson, C., Joly, M., Moutaka, J., Pelat, D., & Serote Roos, M., 2000, *A&A*, 357, 850
- Bothun, G. & Cornell, M., 1990, *AJ*, 99, 1004
- Cid Fernandes, R., Heckman, T., Schmitt, H., Delgado, R. M. G., & Storchi-Bergmann, T. 2001, *ApJ*, 558, 81
- Corbett, E. A., Kewley, L., Appleton, P. N., et al., 2002, *ApJ*, 583, 670
- da Costa, L. N., Geller, M. J., Pellegrini, P. S., et al., 1994, *ApJL*, 424, L1
- da Costa, L. N. Willmer, C. N. A., Pellegrini, P. S., et al., 1998, *AJ*, 116, 1
- Coziol, R., Torres, C. A. O., Quast, G. R., Contini, T., & Davoust, E., 1998, *ApJs*, 119, 239
- Dultzin-Hacyan, D., Krongold, Y., Fuentes-Guridi, I., & Marziani, P., 1999, *ApJL*, 513, L111
- González Delgado, R. M., Heckman, T., & Leitherer, C., 2001, *ApJ*, 546, 845
- de Grijp, M. H. K., Lub, J., & Miley, G. K. 1987, *A&AS*, 70, 95
- Gu, Q., Dultzin-Hacyan, D., & de Diego, J. A. 2001, *RMxAA*, 37, 3
- Hernández Toledo, H. M., Dultzin-Hacyan, D., & Sulentic, J. W. 2001, *AJ*, 121, 1319
- Ho, L. C., 2005, Proceedings of meeting "Extreme Starburst: Near and Far", Lijiang, China (astro-ph/0511157)
- Ho, L. C., Filippenko, A. V., & Sargent, W. L. 1995, *ApJs*, 98, 477
- Huchra, J., 1990, Center for Astrophysics Redshift Catalogue.
- Hunt L. K. & Malkan M. A. 1999, *ApJ*, 516, 660
- Kauffmann, G., Heckman, T.M., Tremonti, C., et al. 2003, *MNRAS*, 346, 1055
- Kim, D.-C., Sanders, D. B., Veilleux, S., Mazzarella, J. M., & Soifer, B. T. 1995, *ApJs*, 98, 129
- Kim, M., Ho, L.C., & Im, M. 2006, *ApJ*, 642, 702
- Kinney, A. L., Bohlin, R. C., Calzetti, D., Panagia, N., & Wyse, R. F. G. 1993, *ApJs*, 86, 5
- Komossa, S., Böhringer, H., & Huchra, J. P. 1999, *A&A*, 349, 88
- Koulouridis, E., Plionis, M., Chavushyan, V., Dultzin-Hacyan, D., Krongold, Y., & Goudis, C. 2006, *ApJ*, 639, 37

- Krongold, Y., Dultzin-Hacyan, D., & Marziani, P. 2002, *ApJ*, 572, 169
- Krongold, Y., Dultzin-Hacyan, D., Marziani, P., & de Diego, J. A. 2003, *RMxAA*, 39, 225
- Marzke, R.O., Huchra, J.P., & Geller, M.J., 1994, *ApJ*, 428, 43
- Mirabel, I. F. & Sanders, D. B. 1988, *ApJ*, 335, 104
- Nicastro, F. 2000, *ApJl*, 530, L65
- Oliva, E., Origlia, L., Maiolino, R., & Moorwood, A. F. M. 1999, *A&A*, 350, 9
- Sanders, D. B., Egami, E., Lipari, S., Mirabel, I. F., & Soifer, B. T. 1995, *AJ*, 110, 1993
- Sanders, D. B., Surace, J. A., & Ishida, C. M. 1999, *IAU Symp.* 186: Galaxy Interactions at Low and High Redshift, 186, 289
- Sanders, D. B., Mazzarella, J. M., Kim, D.-C., Surace, J. A., & Soifer, B. T. 2003, *AJ*, 126, 1607.
- Saraiva, M. F., Bica, E., Pastoriza, M. G., & Bonatto, C. 2001, *A&A*, 376, 43
- Serber, W., Bahcall, N., Menard, B., & Richards, G. 2006, *ApJ*, accepted ([astro-ph/0601522](#))
- Siebenmorgen, R., Haas, M., Krügel, E., & Schulz, B. 2005, *A&A*, 436, L5
- Soifer, B. T., Boehmer, L., Neugebauer, G., & Sanders, D. B. 1989, *AJ*, 98, 766
- Sosa-Brito, R. M., Tacconi-Garman, L. E., Lehnert, M. D., & Gallimore, J. F. 2001, *ApJs*, 136, 61
- Surace, J. A., Sanders, D. B., & Mazzarella, J. M. 2004, *AJ*, 127, 3235
- Tran, H. D. 2003, *ApJ*, 583, 632
- Veilleux, S., Goodrich, R. W., & Hill, G. J. 1997, *ApJ*, 477, 631
- Wang, J. L., Xia, X. Y., Mao, S., Cao, C., Wu, H., & Deng, Z. G. 2006, *ApJ*, submitted ([astro-ph/0603574](#))
- Willmer, C.N.A., da Costa, L.N. & Pellegrini, P.S., 1998, *AJ*, 115, 869
- Zickgraf, F.-J., Voges, W., Krautter, J. et al. 1997, *A&A*, 323, 21

TABLE 1
OUR BRIGHT IRAS SAMPLE GALAXIES WHICH RESIDE IN THE SKY REGION COVERED BY THE
SSRS AND CFA2 CATALOGUES.

NAME	RA (J2000)	DEC (J2000)	m_B	z	D (h^{-1} kpc)	TYPE
NGC0023	00 09 53.1	25 55 25	12.50	0.0152	isolated	starburst
ESO079-G003	00 14 54.7	-39 11 19	12.50	0.0090	isolated	normal
NGC0174	00 36 59.0	-29 28 40	13.62	0.0116	isolated	starburst
UGC00556	00 54 49.6	29 14 43	15.30	0.0154	isolated	Liner
UGC00903	01 21 47.1	17 35 34	14.70	0.0084	isolated	unclassified
ESO353-G020	01 34 51.6	-36 08 08	13.95	0.0161	isolated	normal
NGC0716	01 52 59.3	12 42 31	14.00	0.0152	isolated	normal
UGC01451	01 58 29.9	25 21 34	14.30	0.0164	isolated	normal
NGC0835	02 09 24.5	-10 08 06	13.14	0.0138	11.00	starburst
NGC0838	02 09 38.3	-10 08 45	14.22	0.0128	27.82	starburst
NGC0839	02 09 42.8	-10 10 59	14.20	0.0128	27.91	starburst
NGC0873	02 16 32.2	-11 20 52	12.83	0.0134	isolated	starburst
NGC0877	02 17 58.5	14 32 53	12.50	0.0131	isolated	starburst
NGC0922	02 25 04.4	-24 47 15	12.63	0.0103	isolated	starburst
NGC0992	02 37 25.2	21 06 06	13.50	0.0138	30.32	starburst
NGC1083	02 45 40.5	-15 21 24	15.19	0.0137	isolated	starburst
NGC1134	02 53 40.9	13 00 58	13.20	0.0121	77.18	normal
UGC02403	02 55 57.2	00 41 36	13.20	0.0139	isolated	starburst
NGC1204	03 04 39.9	-12 20 25	14.21	0.0143	isolated	starburst
ESO420-G013	04 13 49.5	-32 00 23	13.52	0.0121	isolated	Sy2
NGC1614	04 31 35.5	-08 40 56	12.00	0.0160	2.00	starburst
NGC2782	09 14 05.5	40 06 54	12.66	0.0085	isolated	starburst
NGC1667	04 46 10.5	-06 24 24	13.00	0.0150	isolated	Sy2
NGC2785	09 15 15.8	40 55 08	14.90	0.0088	52.00	starburst
NGC2856	09 24 16.9	49 14 58	13.90	0.0088	26.53	starburst
NGC3147	10 16 55.8	73 24 07	11.52	0.0094	isolated	Sy2
NGC3221	10 22 21.0	21 34 12	14.30	0.0137	isolated	normal
NGC3367	10 46 34.5	13 45 10	12.22	0.0101	isolated	unclassified
NGC3508	11 02 59.6	-16 17 17	13.20	0.0130	isolated	starburst
NGC3690	11 28 32.9	58 33 19	13.20	0.0104	2.16	starburst
NGC3735	11 36 01.0	70 32 06	12.60	0.0090	isolated	Sy2
NGC3994	11 57 37.0	32 16 39	13.68	0.0105	18.17	Liner
NGC3995	11 57 44.9	32 17 42	12.96	0.0109	18.65	starburst
NGC4175	12 12 30.7	29 10 10	14.20	0.0131	17.39	Sy2
NGC4194	12 14 10.1	54 31 34	13.00	0.0084	isolated	starburst
NGC4332	12 22 47.8	65 50 36	13.20	0.0091	isolated	starburst
NGC4388	12 25 46.7	12 39 40	12.20	0.0084	isolated	Sy2
NGC4433	12 27 38.6	-08 16 49	12.90	0.0099	63.09	normal
MCG-02-33-098	13 02 19.8	-15 46 07	15.38	0.0159	isolated	starburst
MCG-03-34-014	13 12 34.5	-17 32 28	13.02	0.0092	isolated	normal
NGC5020	13 12 40.1	12 35 57	13.40	0.0112	isolated	normal
IC0860	13 15 03.7	24 37 05	14.80	0.0129	isolated	unclassified
NGC5073	13 19 21.4	-14 51 46	13.50	0.0091	isolated	starburst
IC4280	13 32 53.0	-24 12 29	13.51	0.0163	93.52	starburst
NGC5371	13 55 40.3	40 27 38	11.59	0.0085	isolated	unclassified
NGC5394	13 58 33.7	37 27 10	13.85	0.0116	19.44	starburst
NGC5395	13 58 37.9	37 25 27	12.47	0.0116	19.10	Liner
NGC5430	14 00 45.7	59 19 46	13.08	0.0099	isolated	starburst
NGC5433	14 02 36.1	32 30 35	14.00	0.0145	isolated	starburst
NGC5427	14 03 25.7	-06 01 53	11.93	0.0087	22.81	Sy2
NGC5595	14 24 13.2	-16 43 28	13.12	0.0090	32.63	normal
NGC5597	14 24 27.2	-16 45 50	13.32	0.0089	32.68	starburst
NGC5653	14 30 10.3	31 12 50	13.39	0.0119	isolated	starburst
NGC5728	14 42 23.6	-17 15 14	12.81	0.0095	isolated	Sy2
NGC5757	14 47 46.2	-19 04 45	13.50	0.0089	isolated	starburst
NGC5793	14 59 24.6	-16 41 38	14.17	0.0117	37.36	Sy2
UGC09668	14 55 56.0	83 31 29	13.80	0.0131	63.55	starburst
CGCG049-057	15 13 13.2	07 13 26	15.50	0.0130	isolated	starburst
NGC5900	15 15 05.0	42 12 28	15.00	0.0084	70.48	normal
NGC5930	15 26 07.8	41 40 30	13.00	0.0087	3.59	starburst
NGC5936	15 30 01.1	12 59 21	13.41	0.0134	isolated	starburst
NGC5937	15 30 46.0	-02 49 49	13.35	0.0095	isolated	starburst
NGC5990	15 46 16.0	02 24 49	13.10	0.0128	84.90	Sy2
NGC6052	16 05 13.1	20 32 27	14.70	0.0151	isolated	starburst
ESO402-G026	21 22 31.7	-36 40 57	13.69	0.0093	isolated	normal
NGC7130	21 48 19.5	-34 57 10	13.33	0.0161	isolated	unclassified
NGC7172	22 02 02.2	-31 52 15	12.95	0.0086	46.75	Sy2
IC5179	22 16 09.3	-36 50 43	12.46	0.0114	isolated	starburst
ESO534-G009	22 38 41.7	-25 51 02	13.55	0.0113	86.40	Liner
NGC7469	23 03 15.5	08 52 24	13.00	0.0162	18.76	unclassified
NGC7541	23 14 43.0	04 32 03	12.70	0.0089	23.62	starburst
NGC7591	23 18 16.0	06 35 08	13.80	0.0165	isolated	Sy2
NGC7678	23 28 27.7	22 25 15	12.70	0.0116	isolated	Sy2
NGC7714	23 36 14.0	02 09 17	13.10	0.0093	16.12	starburst
NGC7769	23 51 04.7	20 09 03	13.10	0.0141	2.64	unclassified
NGC7771	23 51 24.7	20 06 41	13.39	0.0143	13.23	unclassified
UGC12914	24 01 38.0	23 29 04	13.20	0.0146	14.82	unclassified
UGC12195	24 01 42.2	23 29 41	13.90	0.0145	14.33	unclassified

TABLE 2
THE SUBSAMPLE OF BIRG GALAXIES IN OUR SPECTROSCOPIC SURVEY. BELOW EACH BIRG WE LIST ALL THEIR NEIGHBORS WITHIN A PROJECTED DISTANCE OF $100 h^{-1}$ KPC WITH THEIR MEASURED REDSHIFTS.

NAME	RA J2000	DEC J2000	O_{MAPS} integrated	z	TYPE
NGC0023	00 09 53.1	25 55 25	13.95	0.0152	starburst
none					
UGC00556	00 54 49.6	29 14 43	15.63	0.0154	Liner
neighbor 1	00 54 51.1	29 16 25	17.03	0.0152 \pm 0.0002	
NGC0716	01 52 59.3	12 42 31	14.51	0.0152	Normal
none					
UGC01451	01 58 29.9	25 21 34	15.41	0.0164	Normal
none					
NGC0835	02 09 24.5	-10 08 06	13.67*	0.0138	starburst
neighbor 1	02 09 20.9	-10 08 00	*	0.0130 \pm 0.0002	
neighbor 2	02 09 38.3	-10 08 45	14.89	0.0133 \pm 0.0004	
neighbor 3	02 09 42.8	-10 10 59	15.01	0.0132 \pm 0.0004	
NGC0877	02 17 58.5	14 32 53	13.07	0.0131	starburst
neighbor 1	02 17 53.3	14 31 17	16.04	0.0136 \pm 0.0007	
neighbor 2	02 17 26.3	14 34 49	16.77	0.013376 $\dagger\dagger$	
NGC0922	02 25 04.4	-24 47 15	13.25	0.0103	starburst
neighbor 1	02 24 30.0	-24 44 44	16.73	0.1054 $\dagger\dagger$	
NGC0992	02 37 25.2	21 06 06	15.39	0.0138	starburst
neighbor 1	02 37 28.2	21 08 31	16.99	0.0126 \pm 0.0004	
NGC1614	04 31 35.5	-08 40 56	14.55	0.0160	Sy2
neighbor 1	04 31 35.5	-08 40 56	16.44	0.0160	
NGC1667	04 46 10.5	-06 24 24	13.00 \dagger	0.0160	Sy2
none					
UGC02403	02 55 57.2	00 41 36	15.33	0.0139	starburst
neighbor 1	02 55 58.9	00 40 26	19.10	0.0749 \pm 0.0002	
NGC2785	09 15 15.8	40 55 08	14.85	0.0088	starburst
neighbor 1	09 15 33.8	40 55 27	14.54	0.0653 \pm 0.0004	
neighbor 2	09 14 43.1	40 52 47	14.54	0.008319 $\dagger\dagger$	
neighbor 3	09 14 35.6	40 55 24	17.58	0.008933 $\dagger\dagger$	
NGC2856	09 24 16.9	49 14 58	14.71	0.0088	starburst
neighbor 1	09 24 03.1	49 12 16	14.52	0.0089 \pm 0.0004	
NGC3221	10 22 21.0	21 34 12	13.87	0.0137	Normal
neighbor 1	10 22 26.0	21 32 31	17.06	0.0117 \pm 0.0004	
neighbor 2	10 22 21.1	21 31 00	17.89	0.0539 \pm 0.0003	
neighbor 3	10 22 13.4	21 30 42	18.67	0.0128 \pm 0.0007	
NGC3690	11 28 32.9	58 33 19	13.76*	0.0104	starburst
neighbor 1	11 28 33.5	58 33 47	*	0.010411 $\dagger\dagger$	
neighbor 2	11 28 27.3	58 34 42	*	0.0132 \pm 0.0001	
neighbor 3	11 28 45.8	58 35 36	16.14	0.0604 \pm 0.0002	
NGC4388	12 25 46.7	12 39 40	12.79	0.0084	Sy2
neighbor 1	12 25 41.7	12 48 38	14.50	0.0021 \pm 0.0001	
neighbor 2	12 25 15.2	12 42 53	15.87	<0.001 $\dagger\dagger$	
IC0860	13 15 03.7	24 37 05	15.31	0.0129	unclassified
none					
NGC5073	13 19 21.4	-14 51 46	14.03	0.0091	starburst
neighbor 1	13 19 34.1	-14 46 22	16.21	0.0350 \pm 0.0006	
neighbor 2	13 18 56.4	-14 54 13	16.41	0.0347 \pm 0.0001	
NGC5433	14 02 36.1	32 30 35	14.68	0.0145	starburst
neighbor 1	14 02 39.0	32 27 50	18.00	0.0142 \pm 0.0008	
neighbor 2	14 02 20.5	32 26 53	16.17	0.00141 \pm 0.0007	
NGC5653	14 30 10.3	31 12 50	14.10	0.0119	starburst
none					
NGC5990	15 46 16.0	02 24 49	14.29	0.0128	starburst
neighbor 1	15 46 28.9	02 23 09	18.16	0.0468 \pm 0.0002	
neighbor 2	15 46 23.2	02 21 34	17.58	0.0480 \pm 0.0003	
neighbor 3	15 45 45.9	02 24 35	15.87	0.0141 \pm 0.0001	
NGC7541	23 14 43.0	04 32 03	13.22	0.0089	starburst
neighbor 1	23 14 34.5	04 29 54	14.70	0.0080 \pm 0.0006	
NGC7714	23 36 14.0	02 09 17	13.10 \dagger	0.0093	starburst
neighbor 1	23 36 22.1	02 09 24	14.90 \dagger	0.0089 \pm 0.0001	
NGC7771	23 51 24.7	20 06 41	13.81*	0.0143	unclassified
neighbor 1	23 51 22.5	20 05 47	*	0.0145 \pm 0.0008	
neighbor 2	23 51 13.1	20 06 12	17.13	0.013679 $\dagger\dagger$	
neighbor 3	23 51 04.0	20 09 02	14.05	0.0139 \pm 0.0003	
neighbor 4	23 51 13.9	20 13 46	17.02	0.043527 $\dagger\dagger$	

\dagger Zwicky blue magnitude (Region Not Covered by MAPS Catalog)

$\dagger\dagger$ Redshift from NED

* Not resolved neighboring galaxies

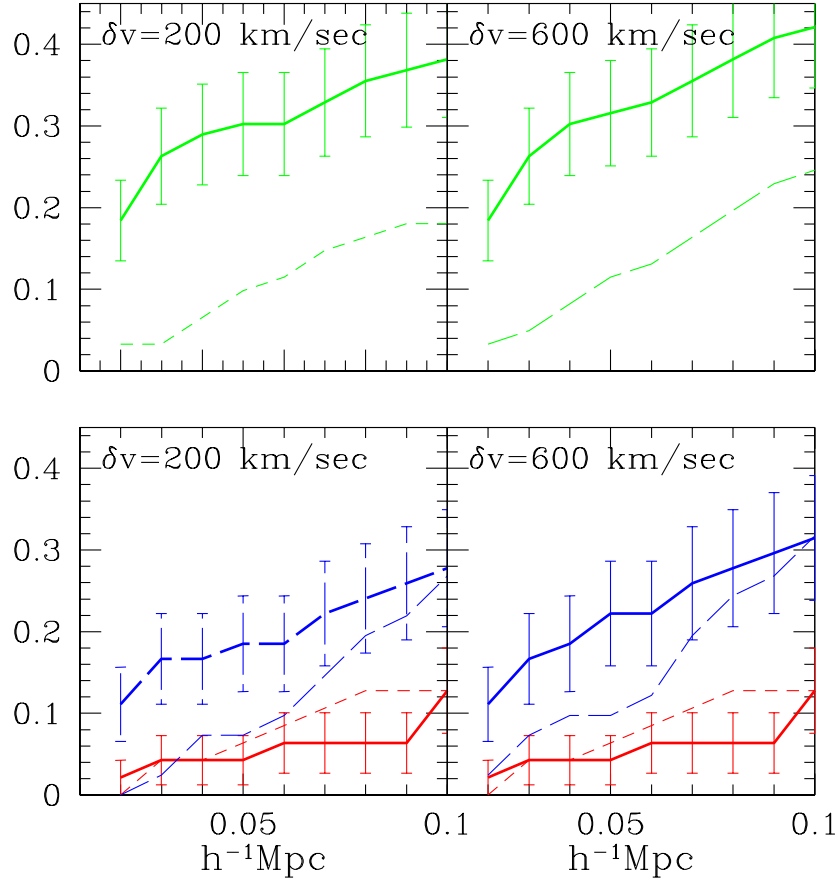


FIG. 1.— *Top Panels:* Fraction of BIRGs (thick line) and their control sample galaxies (thin dashed line) which have their nearest neighbor, within the indicated redshift separation, as a function of projected distance. *Bottom Panels:* Corresponding Sy1 (red) and Sy2 (blue) fractions by Koulouridis et al. 2006

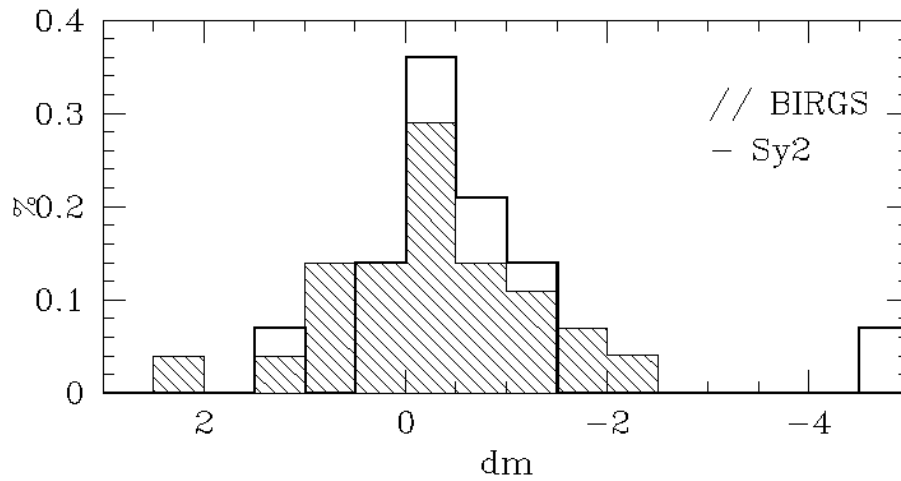


FIG. 2.— The frequency distribution of host (BIRG or Sy2) - nearest neighbor magnitude differences.

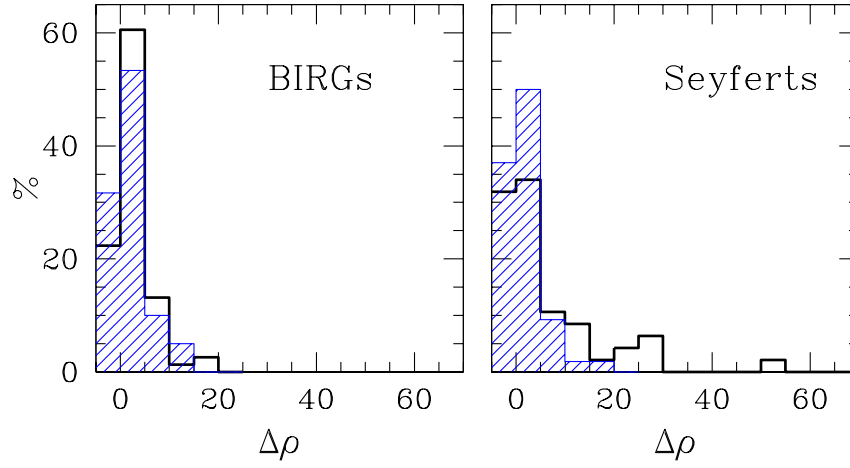


FIG. 3.— *Left Panel:* Frequency distribution of galaxy overdensities around BIRGs (solid line) and control sample (shaded histogram). *Right Panel:* Corresponding distribution around Sy1s (solid line) and Sy2s (dashed histogram). Note that here we do not present the corresponding distributions of their control samples (to this end see Koulouridis et al. 2006).

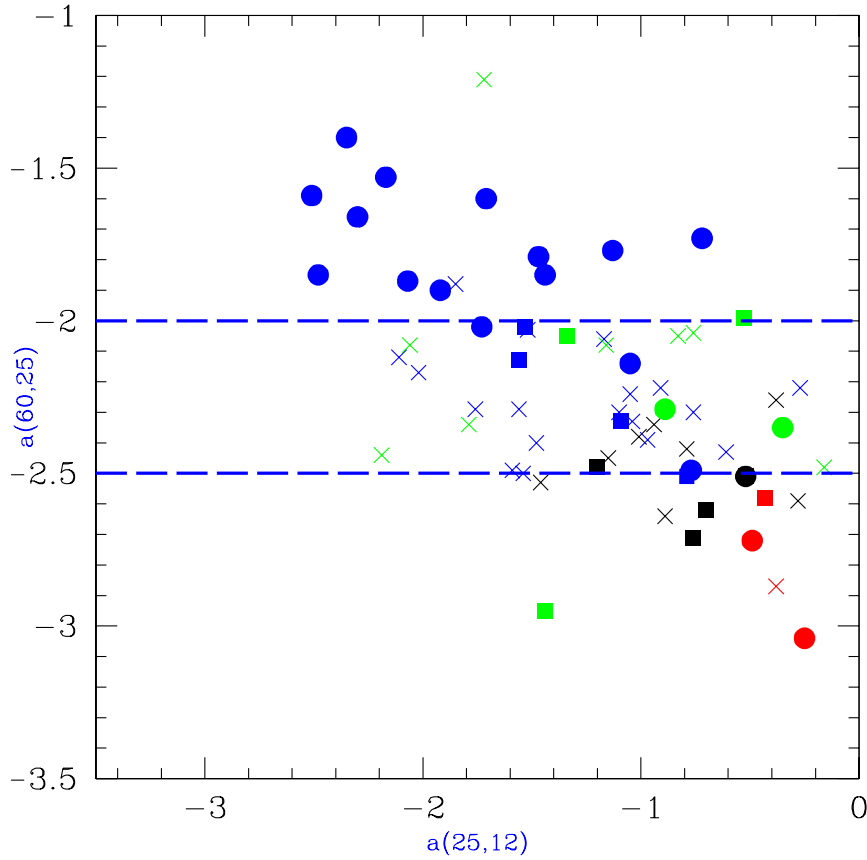


FIG. 4.— FIR color-color diagram: $\alpha(60,25)$ versus $\alpha(25,12)$. The color coding is such that starbursts are represented by blue, Sy2s by green, Liners by red and normal galaxies by black. Highly interacting BIRGs are represented by filled circles, weakly interacting by filled squares and non-interacting by crosses.